Temperature dependence of the acoustoelectric current in graphene

L. Bandhu and G. R. Nash

Citation: Applied Physics Letters **105**, 263106 (2014); doi: 10.1063/1.4905222

View online: http://dx.doi.org/10.1063/1.4905222

View Table of Contents: http://scitation.aip.org/content/aip/journal/apl/105/26?ver=pdfcov

Published by the AIP Publishing

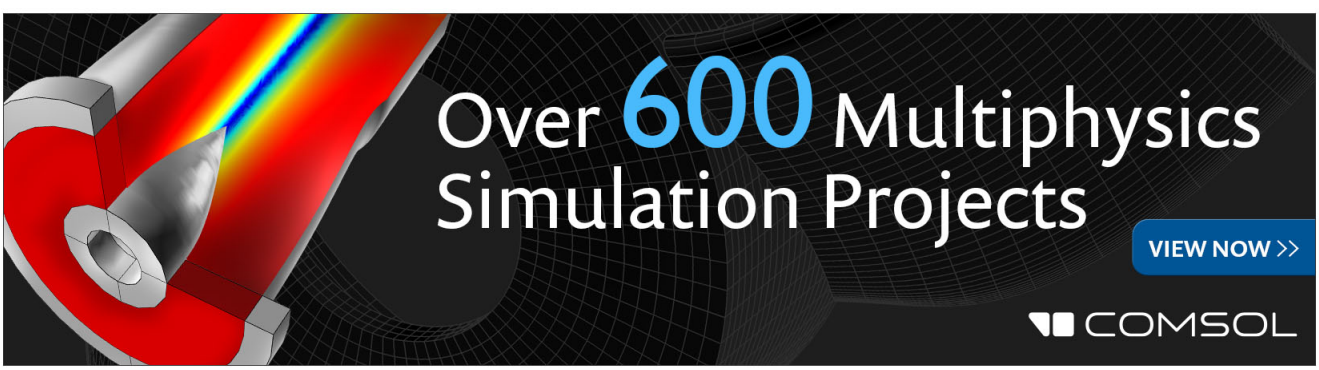

Temperature dependence of the acoustoelectric current in graphene

L. Bandhu and G. R. Nash[a)]
College of Engineering, Mathematics and Physical Sciences, University of Exeter, Exeter EX4 4QF, United Kingdom

(Received 11 November 2014; accepted 17 December 2014; published online 31 December 2014; publisher error corrected 16 January 2015)

The acoustoelectric current in graphene has been investigated as a function of temperature, surface acoustic wave (SAW) intensity, and frequency. At high SAW frequencies, the measured acoustoelectric current decreases with decreasing temperature, but remains positive, which corresponds to the transport of holes, over the whole temperature range studied. The current also exhibits a linear dependence on the SAW intensity, consistent with the interaction between the carriers and SAWs being described by a relatively simple classical relaxation model. At low temperatures and SAW frequencies, the measured acoustoelectric current no longer exhibits a simple linear dependence on the SAW intensity, and the direction of the acoustoelectric current is also observed to reverse under certain experimental conditions. © *2014 AIP Publishing LLC*.
[http://dx.doi.org/10.1063/1.4905222]

Surface acoustic waves (SAWs) have been used extensively over the last few decades as a contactless probe to study the electronic properties of nanostructures such as quantum wires and dots.[1,2] In addition, the transfer of momentum[3,4] from the wave to charge carriers via the piezoelectric interaction can be used to trap and transport charge over macroscopic distances. This effect has been exploited as a means, for example, of storing light in quantum wells[5] and generating and manipulating single electrons and photons, particularly for metrology and quantum information processing.[6–8] Recently, acoustoelectric charge transport has been investigated in graphene,[9,10] and we have previously reported acoustoelectric charge transport at room temperature in large area graphene, transferred onto lithium niobate, between contacts up to 500 μm apart.[11] Using double finger inter-digital transducers (IDTs), we characterised the acoustoelectric current as a function of both SAW intensity and frequency, and at all SAW frequencies a positive acoustoelectric current was observed in the direction of SAW, indicating the transport of holes; consistent with the fact that CVD graphene is thought to be p-doped by water,[12] and the PMMA residues and etchant salts arising from the transfer process.[13] We also showed that these room temperature results were consistent with the attenuation of the SAW being described by a relatively simple classical relaxation model.[14]

In this manuscript, we report measurements of the acoustoelectric current in the same devices as a function of temperature, and also of SAW intensity and frequency. At high SAW frequencies, the direction of the acoustoelectric current remains consistent with the transport of holes over the temperature range studied. However, for low SAW frequencies at low temperature, and also at low SAW intensities, the direction of the acoustoelectric current reverses, consistent with the net transport of electrons. We believe that the very different behaviour observed at different SAW frequencies, corresponding to different SAW wavelengths, reflects the different length scales over which the SAW probes the electronic properties of the graphene.

Commercially available CVD graphene grown on copper was transferred in-between two identical, double-finger IDTs on 128° YX lithium niobate SAW delay lines. The IDTs, which had a transducer aperture of 3.25 mm, define an acoustic path length of 5.2 mm and were designed to give resonances at a number of frequencies. Graphene was transferred following the standard PMMA transfer technique,[15] with Raman spectroscopy used to confirm that it was single layer. E-beam lithography and thermal evaporation were used to define relatively large area contacts (3 mm × 20 μm), consisting of 7 nm Cr and 70 nm Au, on top of the graphene (see Figure 1). All measurements were made between contacts C and D that were 300 μm apart. Further details of the sample fabrication and characterisation can be found in Ref. 11.

Samples were bonded to a printed circuit board (PCB), using a conductive silver epoxy, which was then mounted on the cold-finger of a close-cycle cryostat and measurements were undertaken at different temperatures, with the chamber evacuated to a pressure of approximately 3.6×10^{-6} mbar. The conductivity of the graphene was measured using a two terminal current-voltage measurement, with no SAW present. For acoustoelectric measurements, a continuous SAW was excited at the input transducer using an Agilent 8648C RF signal generator, and the SAW amplitude was measured

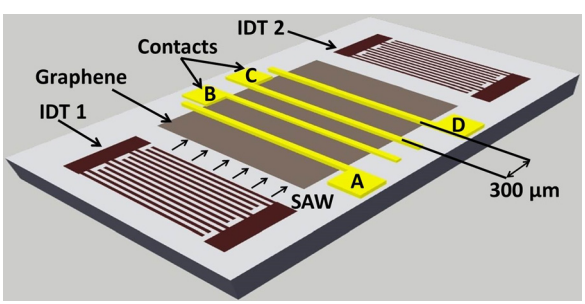

FIG. 1. Schematic diagram of the device layout.

[a)]Author to whom correspondence should be addressed. Electronic mail: g.r.nash@exeter.ac.uk

at the output transducer using a LeCroyWaveRunner digital oscilloscope. A Keithley 2400 source-measurement unit (SMU) was used to measure the acoustoelectric current (I_{ae}) generated in the graphene (no bias was applied between the contacts).

In Figure 2, the acoustoelectric current measured as a function of SAW intensity and temperature is plotted for a SAW frequency of 269 MHz. At this frequency, which corresponds to a SAW wavelength of approximately 15 μm, a positive acoustoelectric current was observed in the direction of SAW at all temperatures, although the size of the measured acoustoelectric current decreases with decreasing temperature (note that at temperatures below 95 K, the measured acoustoelectric current begins to increase slightly with decreasing temperature. However, at a SAW intensity of 0.02 W/m, for example, the measured current at 48 K is still approximately 35× smaller than that measured at 300 K). The straight lines shown in Figure 2 are least square linear fits to the measured data, where we have taken the acoustoelectric current density j (Refs. 3 and 4) to be given by

$$j = -\mu Q = \mu \frac{I\Gamma}{v}, \tag{1}$$

where μ is the carrier mobility and Q is the phonon pressure given by $Q = \frac{I\Gamma}{v}$, and I is the SAW intensity, Γ is the attenuation coefficient, and v is the velocity of the wave (approximately 4000 m/s). In this model, the acoustoelectric current therefore depends linearly upon the SAW intensity, as observed in the measured data, and the linear fitting was carried out using the mobility as the fitting parameter. The attenuation coefficients at each temperature were calculated using the measured values of the conductivity (which are plotted in Figure 3(a)) and by assuming that the piezoelectric interaction between the SAWs and charge carriers is described by a simple classical relaxation model,[14] such that the attenuation per unit length (Γ) is a non-monotonic function of the diagonal component of the conductivity tensor σ^{2D}

$$\Gamma = K_{eff}^2 \frac{\pi}{\lambda}\left[\frac{(\sigma^{2D}/\sigma_M)}{1+(\sigma^{2D}/\sigma_M)^2}\right], \tag{2}$$

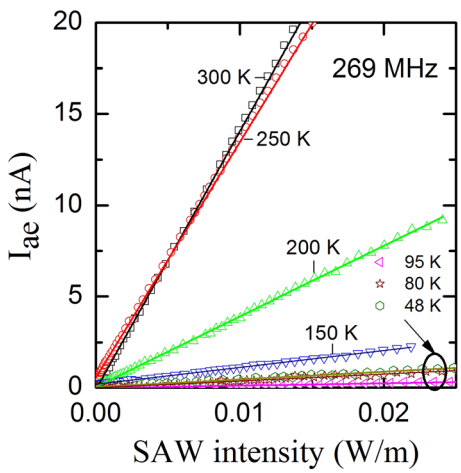

FIG. 2. Measured acoustoelectric current (symbols) as a function of SAW intensity and temperature for a SAW frequency of 269 MHz. The straight lines are least square linear fits to the measured data.

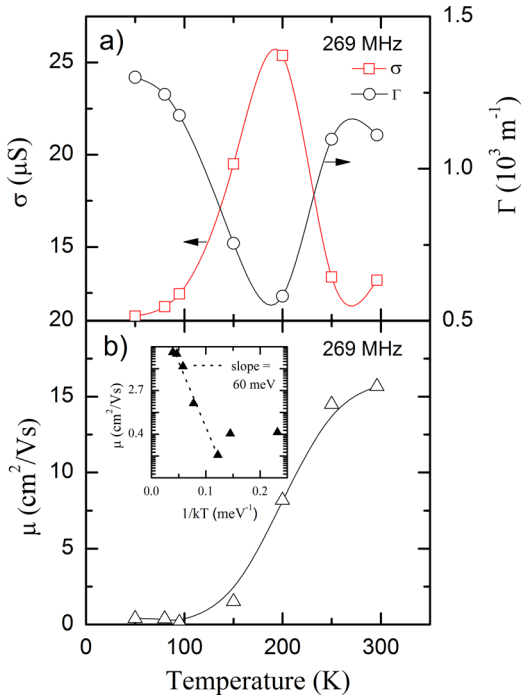

FIG. 3. (a) Measured conductivity and calculated values of attenuation coefficient. (b) Values of mobility taken to simulate measured data at 269 MHz, plotted as a function of temperature. The inset is of an Arrhenius lot of the extracted mobility values.

where λ is the SAW wavelength, K_{eff}^2 is the piezoelectric coupling coefficient (0.056 for lithium niobate), and the attenuation coefficient has a maximum at a characteristic conductivity σ_M. For a hybrid system based on lithium niobate ($LiNbO_3$), the characteristic conductivity σ_M is approximately given by $\sigma_M = v\varepsilon_0(\sqrt{\varepsilon_{xx}^S \varepsilon_{zz}^S}+1) = 1.25\times10^{-6}\ \Omega^{-1}$,[4] where ε_0 is the permittivity of free space, ε_{xx}^S and ε_{zz}^S are the dielectric constants of $LiNbO_3$ at constant stress. The attenuation coefficients calculated using Eq. (2) are also plotted as a function of temperature in Figure 3(a), with the values of mobility obtained from the fitting plotted in Figure 3(b).

The value of mobility obtained at room temperature is much smaller than the typical room temperature values (~1000 cm^2 V^{-1} s^{-1}) we have extracted from field effect characteristics measured on similar 3 mm × 3 mm devices,[16] where CVD graphene was transferred into Si/SiO_2 substrates. However, as no other values of mobility in CVD graphene transferred onto lithium niobate have been reported, the difference in the mobilities could be due to the different properties of the substrates. In addition, although the measured linear dependence of the acoustoelectric current on SAW intensity and SAW frequency,[11] for high SAW frequencies or at high temperatures, suggests that the relatively simple model of the acoustoelectric transport described above can be used to describe the measurements presented here, it should be noted that the attenuation of the SAW by the charge carriers in the graphene is determined by the conductivity of the graphene on the scale of approximately one half of the SAW wavelength.[17] If the conduction path is inhomogeneous, the values of mobility obtained from this model will therefore depend on the SAW frequency used and may be different to those obtained, for example, from a field effect measurement.

On initial cooling (at temperatures above 200 K), our results suggests that the mobility decreases, whereas the carrier concentration increases. One possible mechanism for this increase in the carrier concentration is the condensation of water, which is a known dopant,[12] onto the surface of the sample as it is initially cooled in the relatively poor vacuum of the cold-finger cryostat. In addition, the conductivity of large-area CVD graphene is known to arise from many competing mechanisms.[18,19] Even at room temperature the conductivity of transferred CVD graphene is known to be spatially inhomogeneous, due to grain boundaries (as the graphene is polycrystalline), tears, wrinkles, and non-homogenous impurities,[20,21] and the potential barriers associated with grain boundaries can lead to thermally activated conductivity[21,22] and mobility.[23] At low temperature, this causes the graphene to tend towards insulating, as observed here (Figure 3(a)). The inset of Figure 3(b) is an Arrhenius plot of the extracted mobility values, where the dotted line is a linear fit to the values in the range of 100 K–300 K. The mobility can therefore be fitted well by an Arrhenius relation, with the mobility $\mu \propto \exp(-E_a/kT)$, where E_a is the activation energy and k is the Boltzmann constant, and an activation energy of 60 meV was obtained from the linear fit shown in the inset. Yazyev and Louie[22] calculated that the potential barriers associated with grain boundaries lie in the range of 0.3 eV–1.4 eV, depending on the structure of the boundary. Song *et al.*[21] and Kumari *et al.*[23] obtained activation energies of 10 meV and 16.2 meV for the measured conductivity of CVD graphene, respectively, which they assigned to the effect of grain boundaries. Kumari *et al.*[23] also obtained a slightly higher value of activation energy, 18.8 meV, from the temperature dependence of the measured mobility. The value of activation energy obtained here is therefore consistent with the conductivity of the CVD graphene, on lithium niobate, also being strongly affected by the presence of grain boundaries.

At high temperatures, the acoustoelectric current measured at lower SAW frequencies also has a linear dependence on the SAW intensity, as shown for SAW frequencies of 32 MHz and 11 MHz in Figures 4(a) and 4(b), respectively, and a positive acoustoelectric current is also observed in the direction of the SAW propagation (note that to allow the results at different frequencies to be compared, we have corrected the SAW intensity using the measured response of the transducer at each temperature at each frequency). In this case, smaller values of mobility (6 $cm^2\ V^{-1}\ s^{-1}$ for 11 MHz at room temperature) have to be used to get good agreement between the calculated and measured values of acoustoelectric current. However, at 269 MHz, one half of the SAW wavelength is approximately 8 μm, which is the order of the size of typical single crystal grains,[21] whereas at 11 MHz half of the SAW wavelength is $\sim$180 μm. The low frequency SAW will therefore be much more sensitive to the effect of grain boundaries in the conductivity, leading to a lower value of the mobility extracted through the SAW measurements. The use of different frequencies SAWs therefore could allow the conductivity of the graphene to be probed over different length scales.

At low temperatures, the measured intensity dependence of the acoustoelectric current at low SAW frequencies is markedly different from that obtained at high frequencies. For SAW frequencies of 32 MHz and 11 MHz, the measured acoustoelectric current no longer shows the simple linear dependence on the SAW intensity as observed at higher temperatures and higher SAW frequencies. Furthermore, at 32 MHz, below 80 K and for SAW intensities below approximately 0.065 W/m, the current reverses direction, indicating that overall the SAW is now transporting more electrons than holes. At 11 MHz, this effect is much more pronounced and for all temperatures below 100 K a negative current is observed at low values of SAW intensity. At low carrier densities and temperatures, the conductivity of the graphene becomes strongly affected by the formation of a large number of electron-hole charge puddles, and an important component of the conductivity will be the percolation of thermally excited "activated" carriers over potential fluctuations in disorder sites (charge puddles or grain boundaries).[18] The low frequency SAW is again likely to be much more sensitive to this due to the relative large length scales over which it probes the conductivity. Moreover, in this regime the SAW itself could influence the conductivity of the graphene, through the transfer of momentum to the carriers, as shown in Eq. (1), leading to the observed non-linear dependence of the current on the SAW intensity.

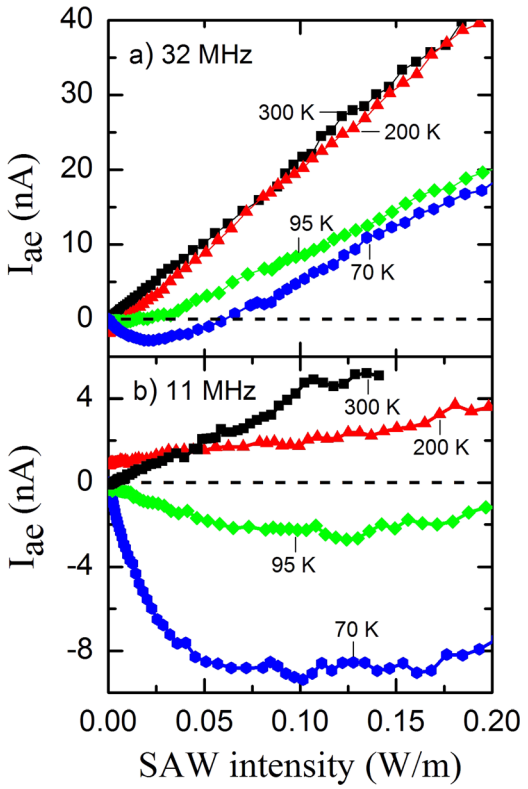

FIG. 4. Measured acoustoelectric current as a function of SAW intensity and temperature for SAW frequencies of (a) 32 MHz and (b) 11 MHz.

Finally, one scenario in which a reversal of the current direction could occur is when the doping of the graphene is due to relatively widely spaced, but high density, puddles of holes superimposed on a relatively low density, but more uniform, density of electrons. Recently, intrinsic spontaneous polarization of hexagonal SiC has been proposed as a possible mechanism of the doping of quasi-free-standing graphene

on the surface of the SiC.[24] Lithium niobate is highly pyroelectric[25] and on cooling it is possible that induced surface charge could cause n-type doping. However, much more work is required to understand this, and also how the use of a different substrate influences the doping of the graphene caused by water.[12] Further work is now underway to investigate the temperature dependence of the acoustoelectric transport in devices, in which the carrier density within the graphene can be varied using an electrostatic gate. This should allow further information to be extracted regarding the different conduction regimes.

In conclusion, we have investigated the temperature dependence of acoustoelectric charge transport in large-area CVD graphene transferred to lithium niobate substrates. At high SAW frequencies, the measured acoustoelectric current decreases with decreasing temperature, but remains positive, which corresponds to the transport of holes, over the whole temperature range. The measured current is also proportional to the SAW intensity over the temperature range, consistent with the attenuation of the SAW by the carriers in the graphene being described using a simple classical relaxation model. The measured acoustoelectric current at low SAW frequencies at high temperatures is also linearly proportional to the SAW intensity, but in this case much lower values of mobility have to be used to give good qualitative agreement between the measured and calculated values of the acoustoelectric current. This suggests that the use of different frequency SAWs with associated different wavelengths allows the conductivity of the graphene to be probed over different length scales. At low temperatures and SAW frequencies, the measured acoustoelectric current no longer exhibits a simple linear dependence on the SAW intensity, and the direction of the acoustoelectric current is observed to reverse under certain experimental conditions. We believe that this is due to the interaction between the SAW and the complex conductivity landscape of the graphene in a percolation regime. However, much more work is required to understand this fully.

The authors would like to acknowledge the financial support of the Royal Society (RG100570).

[1]G. R. Nash, S. J. Bending, M. Boero, P. Grambow, K. Eberl, and Y. Kershaw, Phys. Rev. B **54**, R8337 (1996).
[2]G. R. Nash, S. J. Bending, M. Boero, M. Riek, and K. Eberl, Phys. Rev. B **59**, 7649 (1999).
[3]V. I. Fal'ko, S. V. Meshkov, and S. V. Iordanskii, Phys. Rev. B **47**, 9910 (1993).
[4]M. Rotter, A. Wixforth, W. Ruile, D. Bernklau, and H. Riechert, Appl. Phys. Lett. **73**, 2128 (1998).
[5]C. Rocke, S. Zimmermann, A. Wixforth, J. P. Kotthaus, G. Böhm, and G. Weimann, Phys. Rev. Lett. **78**, 4099 (1997).
[6]O. D. D. Couto, Jr., S. Lazić, F. Iikawa, J. A. H. Stotz, U. Jahn, R. Hey, and P. V. Santos, Nat. Photonics **3**, 645 (2009).
[7]S. Hermelin, S. Takada, M. Yamamoto, S. Tarucha, A. D. Wieck, L. Saminadayar, C. Bauerle, and T. Meunier, Nature **477**, 435 (2011).
[8]A. Hernández-Mínguez, M. Möller, S. Breuer, C. Pfüller, C. Somaschini, S. Lazić, O. Brandt, A. Garcia-Cristóbal, M. M. de Lima, Jr., A. Cantarero, L. Geelhaar, H. Riechert, and P. V. Santos, Nano Lett. **12**, 252 (2012).
[9]V. Miseikis, J. E. Cunningham, K. Saeed, R. O'Rorke, and A. G. Davies, Appl. Phys. Lett. **100**, 133105 (2012).
[10]P. V. Santos, T. Schumann, M. H. Oliveira, J. M. J. Lopes, and H. Riechert, Appl. Phys. Lett. **102**, 221907 (2013).
[11]L. Bandhu, L. M. Lawton, and G. R. Nash, Appl. Phys. Lett. **103**, 133101 (2013).
[12]T. O. Wehling, A. I. Lichtenstein, and M. I. Katsnelson, Appl. Phys. Lett. **93**, 202110 (2008).
[13]A. Pirkle, J. Chan, A. Venugopal, D. Hinojos, C. W. Magnuson, S. McDonnell, L. Colombo, E. M. Vogel, R. S. Ruoff, and R. M. Wallace, Appl. Phys. Lett. **99**, 122108 (2011).
[14]A. Wixforth, J. Scriba, M. Wassermeier, J. P. Kotthaus, G. Weimann, and W. Schlapp, Phys. Rev. B **40**, 7874 (1989).
[15]X. Li, W. Cai, J. An, S. Kim, J. Nah, D. Yang, R. Piner, A. Velamakanni, I. Jung, E. Tutuc, S. K. Banerjee, L. Colombo, and R. S. Ruoff, Science **324**, 1312 (2009).
[16]I. J. Luxmoore, C. Adlem, T. Poole, L. M. Lawton, N. H. Mahlmeister, and G. R. Nash, Appl. Phys. Lett. **103**, 131906 (2013).
[17]M. Levy, J. Schmidt, A. Schenstrom, M. Revzen, A. Ron, B. Shapiro, and C. G. Kuper, Phys. Rev. B **34**, 1508 (1986).
[18]Q. Li, E. H. Hwang, and S. Das Sarma, Phys. Rev. B **84**, 115442 (2011).
[19]J. Heo, H. J. Chung, S.-H. Lee, H. Yang, D. H. Seo, J. K. Shin, U.-I. Chung, S. Seo, E. H. Hwang, and S. Das Sarma, Phys. Rev. B **84**, 035421 (2011).
[20]Y. Zhang, V. W. Brar, C. Girit, A. Zett, and M. F. Crommie, Nat. Phys. **5**, 722 (2009).
[21]H. S. Song, S. L. Li, H. Miyazaki, S. Sato, K. Hayashi, A. Yamada, N. Yokoyama, and K. Tsukagoshi, Sci. Rep. **2**, 337 (2012).
[22]O. V. Yazyev and S. G. Louie, Nat. Mater. **9**, 806 (2010).
[23]A. Kumari, N. Prasad, P. K. Bhatnagar, P. C. Mathur, A. K. Yadav, C. V. Tomy, and C. S. Bhatia, Diamond Relat. Mater. **45**, 28 (2014).
[24]J. Ristein, S. Mammadov, and Th. Seyller, Phys. Rev. Lett. **108**, 246104 (2012).
[25]R. S. Weis and T. K. Gaylord, Appl. Phys. A **37**, 191 (1985).